

Received: 2019.01.06
Accepted: 2019.01.22
Published: 2019.02.02

Atorvastatin Protects Against Cerebral Aneurysmal Degenerative Pathology by Promoting Endothelial Progenitor Cells (EPC) Mobilization and Attenuating Vascular Deterioration in a Rat Model

Authors' Contribution:
Study Design A
Data Collection B
Statistical Analysis C
Data Interpretation D
Manuscript Preparation E
Literature Search F
Funds Collection G

ACEFG 1 **Huijie Wei***
C 1 **Mengchen Yang***
E 1 **Kai Yu**
CE 1 **Wang Dong**
C 1,2 **Wang Liang**
ACE 1 **Zengguang Wang**
BEG 1 **Rongcai Jiang**
ACEG 1 **Jianning Zhang**

1 Department of Neurosurgery, Tianjin Medical University General Hospital; Tianjin Neurological Institute; Key Laboratory of Post-Trauma Neuro-Repair and Regeneration in Central Nervous System, Ministry of Education; Tianjin Key Laboratory of Injuries, Variations and Regeneration of Nervous System, Tianjin, P.R. China
2 Department of Neurosurgery, Peking University International Hospital, Beijing, P.R. China

Corresponding Authors:

* Huijie Wei and Mengchen Yang contributed equally to this work
Huijie Wei, e-mail: huijiwei@126.com, Rongcai Jiang, e-mail: jiang116216@163.com,
Jianning Zhang, e-mail: jianningzhang@hotmail.com

Source of support:

This study was supported by grants 81200907 (HJW), 81671380 (DW), 81671221 (RCJ) and 81720108015(JNZ) from the Chinese Science Foundation (Beijing); grant 12JCQJNC06800 (HJW) from the Tianjin Natural Science Foundation (Tianjin); grant 2018001 (ZGW) from the Tianjin Science and Technology Projects in Key Areas of Traditional Chinese Medicine (Tianjin), and grant 2018ZD03 (ZGW) from the Scientific Research Program Project of Tianjin Education Commission (Tianjin)

Background:

Endothelial injury is the early pathological change of cerebral aneurysm (CA) formation. In addition to its lipid-lowering activity, atorvastatin (ATR) also reportedly promotes vascular repair via mobilizing endothelial progenitor cells (EPC). Here, we investigated the influence of ATR on vascular worsening after CA induction in rats.

Material/Methods:

Adult male Sprague-Dawley rats were randomly assigned to 3 groups: a control (CTR) group, a CA group, and a CA+ATR treatment group. Circulating EPC level and hematological and lipid profiles were measured 3 months after CA induction. Verhoeff-Van Gieson staining and transmission electron microscopy were performed to assess pathological changes in the artery wall. RT-PCR was also performed to evaluate the expression of inflammation-related genes in the aneurysmal wall.

Results:

ATR significantly restored the impaired level of circulating EPC without changing hematological and lipid profiles 3 months after CA induction. ATR markedly inhibited endothelial injury, media thinning, and CA enlargement, accompanied by reduced vascular inflammation.

Conclusions:

Our preliminary results demonstrate that the mobilization of EPC and improvement of endothelial function by ATR contribute to the prevention of cerebral aneurysm. Further studies are warranted to investigate the detailed mechanism.

MeSH Keywords:

Endothelial Cells • Intracranial Aneurysm • Neovascularization, Pathologic • Pathology, Molecular

Full-text PDF:

<https://www.medscimonit.com/abstract/index/idArt/915005>

 2499

 1

 6

 31



Background

The incidence of aneurysmal subarachnoid hemorrhage (SAH) is approximately 10 to 21 in 100 000 individuals per year [1]. The initial mortality within a few days of aneurysmal hemorrhage is 28–40% and the overall mortality and morbidity is greater than 50% [2]. Currently, surgical clipping and endovascular embolization are the main methods used to prevent the rupture of unruptured cerebral aneurysm (CA). However, because many factors (e.g., natural history, patient age, asymptomatic or not, CA size, and CA location) can influence clinical outcomes, the management of unruptured CA is controversial [3].

Histopathologically, the degenerative changes of the CA vessel wall are characterized by endothelial damage, degradation of internal elastic layer (IEL), media thinning caused by excessive apoptosis and phenotypic transition of smooth muscle cells (SMC), inflammatory cells infiltration, and activation of matrix metalloproteinases (MMPs) [4]. Endothelial dysfunction or damage, the earliest pathological change in CA formation, triggers devastating aneurysmal degeneration with the help of abnormal hemodynamic stresses [5]. The level of circulating endothelial progenitor cells (EPC) correlate with endothelial function [6] and EPC can maintain vascular homeostasis and function through neovascularization and re-endothelialization of the injured vessel [7]. Our previous study suggested that decreased level of circulating EPC in CA patients and rats was closely related to the development of CA [8,9]. We further found that EPC transfusion improved endothelial function and attenuated aneurysmal degeneration in a rat model of CA [10]. Evidence indicates that in cardiovascular events, part of the vasculoprotective action of atorvastatin (ATR) is mediated by an improvement in EPC mobilization [11,12]. In the present study we examined the effect of ATR on the level of circulating EPC and its effect on aneurysmal degeneration in rats undergoing CA induction.

Material and Methods

Experimental design and CA induction

All animal work was performed according to US National Institutes of Health's Guide for the Care and Use of Laboratory Animals and was certified by the Institutional Animal Care and Use Committee of the Tianjin Medical University (Ethics approval no. 20160912). We obtained 7-week-old healthy male Sprague-Dawley rats from the Military Medical Academy of China. Induction CA was prepared as formerly described [13]. After rats were deeply anesthetized by 10% chloral hydrate (0.3 ml/0.1 kg, i.p.), we ligated the left common carotid artery and posterior branches of left and right renal arteries. A high-salt diet (8% sodium chloride) was administered starting at

24 h after surgery and continued for 1 month, at which time the experimental CA formed. The surgery and high-salt diet cause and maintain abnormal hemodynamic insults to vascular bifurcations [9].

To investigate the influence of ATR on the progression of pre-existing CA, rats were randomly assigned to 3 groups (Figure 1A) as follows: (1) control (CTR) group (n=16): normal rats did not undergo surgery and were fed only a normal chow diet throughout the course of the experiment; (2) CA group (n=16): rats undergoing surgery were fed a high-salt diet from 24 h to 1 month post-surgery and then were given a normal chow diet for 2 additional months; (3) CA+ATR group (n=16): after 1 month of normal chow diet, CA rats received intragastric administration of ATR (3 mg/kg/day; Pfizer, Ann Arbor, MI, USA) in drinking water every day with a normal diet for 2 extra months. The angiogenesis-promoting effect of this dose of ATR has been proved by a previous study [14]. Without any anesthesia, blood pressure of rats was measured via tail-cuff method (Kent Scientific Corporation, Torrington, USA) at 1, 2, and 3 months after CA induction surgery.

Measurement of circulating EPC level and hematological and lipid profiles

At 3 months after CA induction, peripheral blood samples were collected from the retro-orbital venous plexus. Following Ficoll gradient centrifugation, the obtained mononuclear cells (MNCs) were washed twice in phosphate-buffered saline (PBS) and incubated in blocking buffer for 30 min at 4°C. Then, MNCs were labelled with PE-combined CD34 antibody (Santa Cruz Biotechnology, Santa Cruz, Shanghai, China) and FITC-combined CD133 antibody [15] (Abcam, Cambridge, MA, USA) for 30 min at room temperature. The circulating EPC was defined as CD133- and CD34-positive MNCs and detected by flow cytometry (BD FACS Aris™, Beckman-Dickinson, San Jose, CA, USA) (Figure 1B–1E). Blood cell count and lipid level were measured using a Sysmex XT-1800i hematology analyzer (Sysmex Corporation, Kobe, Japan) and a high-performance liquid chromatography (Polymer 285 Technology System, Inc, Indianapolis, IN), respectively.

Verhoeff-Van Gieson staining

At 3 months post CA induction, the right anterior cerebral artery and olfactory artery (OA/ACA) bifurcations were stripped from euthanized rats (Figure 2A). We performed Verhoeff-Van Gieson staining to evaluate aneurysmal degeneration in the bifurcations (Figure 2B–2D). According to the evaluation system, IEL scores were classified as score 0 (IEL continuous), score 1 (IEL fragmented), and score 3 (IEL completely disappeared) [16]. The media thickness was determined by calculating the percentage of the minimal thickness in the media of

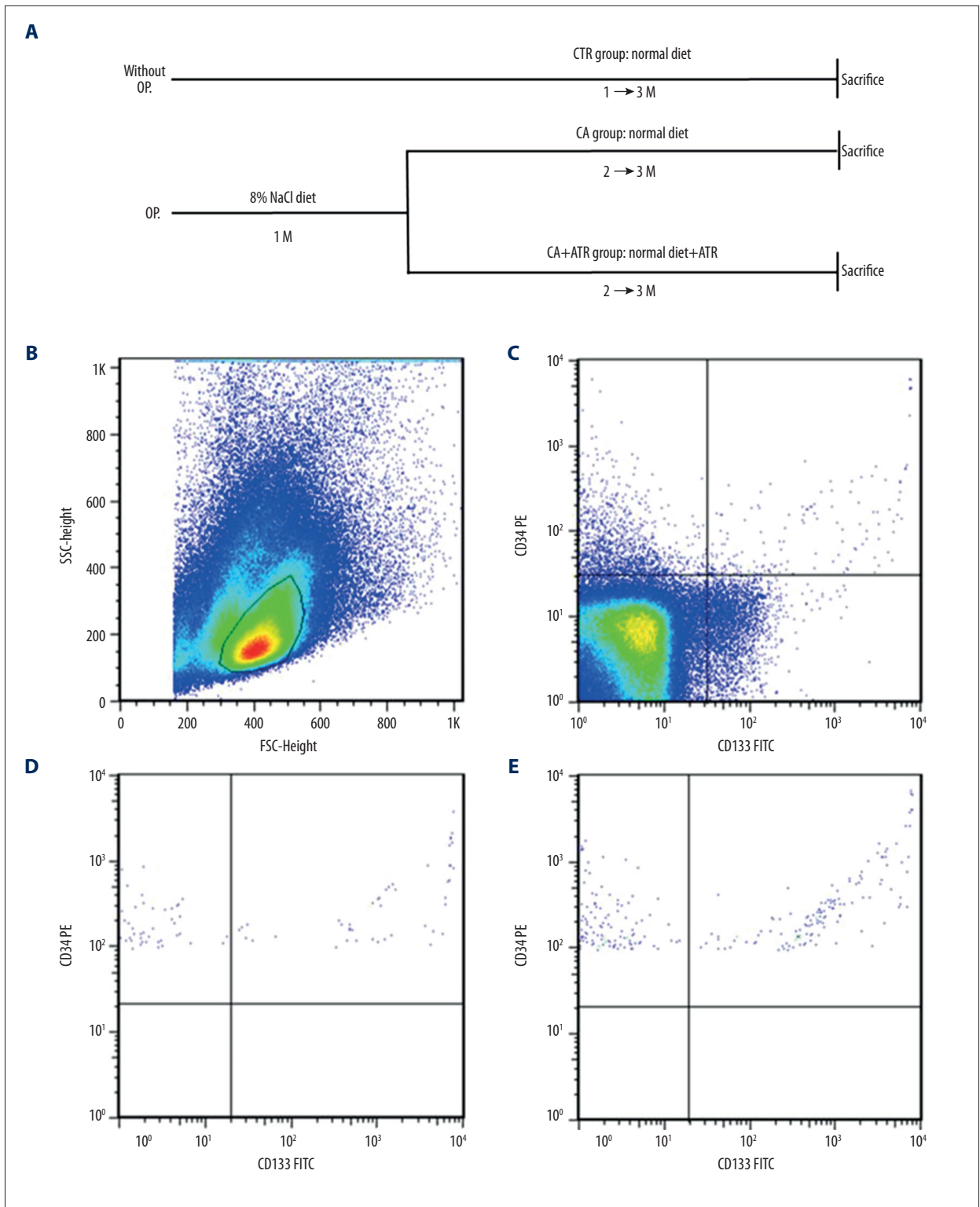


Figure 1. The time course of the experiment (A). A sample illustration of gates setting of CD34/CD133-positive EPC using flow cytometry (B, C). Representative photographs of EPC detection in CA group (D) and CA+ATOR group (E).

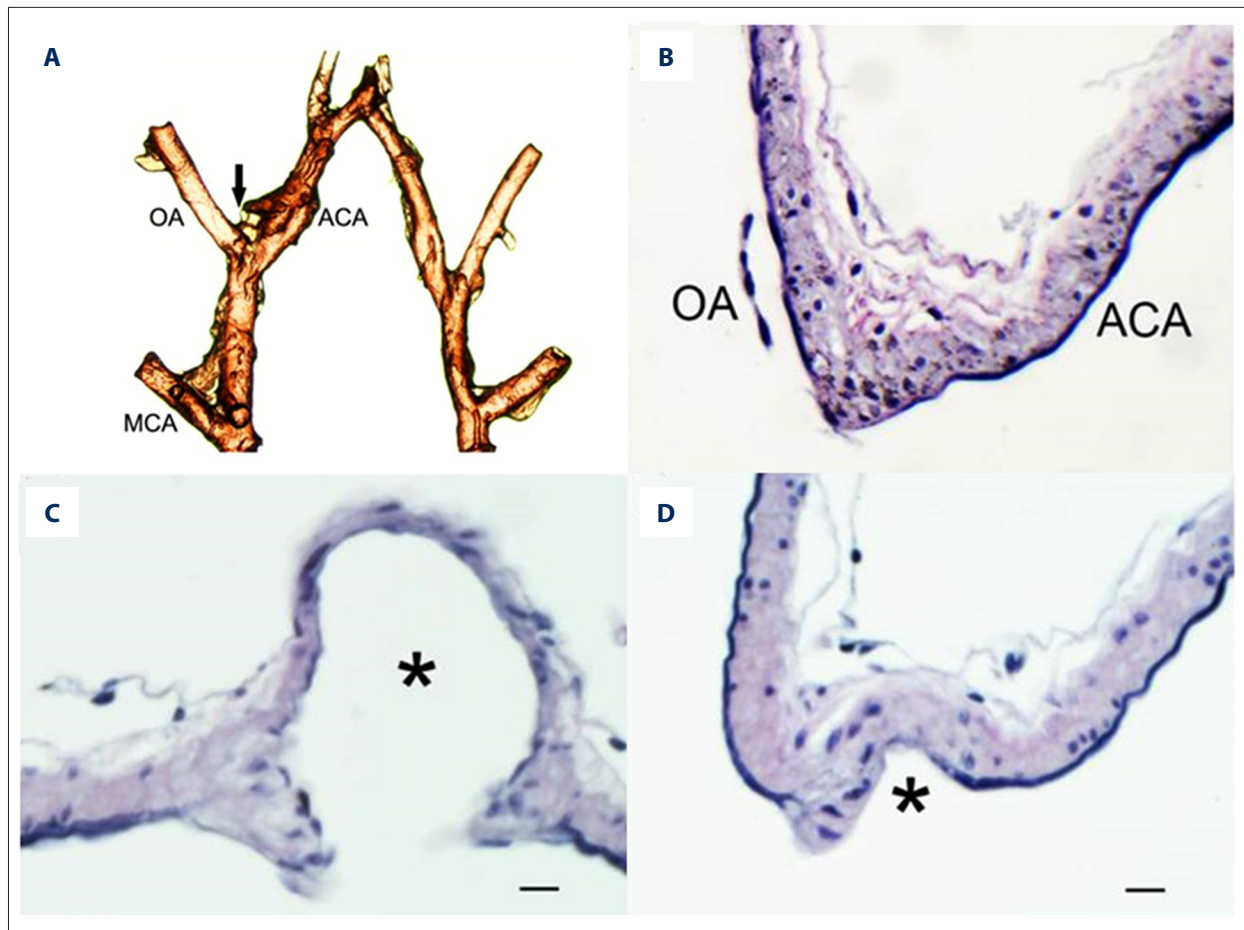


Figure 2. The representative image showing cerebral arteries branches (A). Representative photographs showing the aneurysmal structure change in the right OA/ACA bifurcations 3 months after CA induction surgery (B–D). Arrow shows CA formation at the right anterior cerebral artery/olfactory artery (OA/ACA) bifurcation. MCA – middle cerebral artery. The asterisk indicates aneurysmal lumen (under 10×40 objective lens). Bar=30 μ m.

an aneurysm to the media thickness in the surrounding normal arterial walls. Aneurysm size was expressed as a mean of the maximal longitudinal and transverse diameter.

Transmission electron microscopic observation

We observed the ultrastructure of the aneurysm vascular wall at the right OA/ACA bifurcations at 3 months after CA induction using transmission electron microscopy (TEM). Briefly, dissected right OA/ACA bifurcations were quickly fixed in 3% glutaraldehyde in 0.1 mol/L cacodylic acid buffer (pH 7.2) for 2 h and then post-fixed in 1% osmic acid for 2 h. After dehydration in an ethanol series, tissues were soaked in the mixed liquor of acetone and epoxy resin. Then, tissues were embedded in paraffin and cut into semi-thin (1 μ m) sections. Toluidine blue staining was performed to locate the aneurysmal degeneration of right OA/ACA bifurcations. After positioning, tissues were cut into 100-nm sections using a Leica EM UC7 ultramicrotome (Leica Microsystems, Bannockburn, IL), installed on

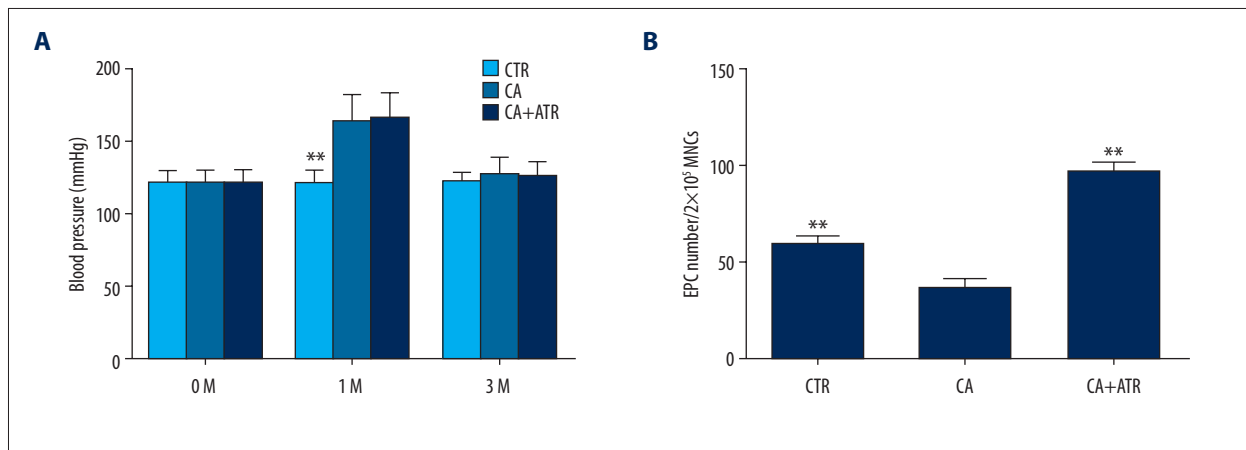
copper grids, and stained with uranyl acetate and lead citrate. Specimens were observed with a Hitachi H-7650 transmission electron microscope (TEM; H-7650, Hitachi, Ltd., Tokyo, Japan).

RT-PCR detection

At 3 months after CA induction, total RNAs from the whole Willis ring tissue were extracted by Trizol reagent (Life Technologies, Grand Island, NY, USA) in accordance with the manufacturer's instructions. RT-PCR was performed using a Takara PrimeScript[®] RT reagent Kit (Takara, Dalian, China) and SYBR Green Realtime PCR Kit (QIAGEN, Hilden, Germany). Primer sequences were: forward 5'-ACGATCTGTTCCCTCATC-3', reverse 5'-TGCTTCTCTCCCAGGAATA-3' for NF- κ B (nuclear factor κ B); 5'-TTCAGGTATGCGGTATTTGG-3' and 5'-GTTGGAAGTGTAGCGTTTCG-3' for iNOS (inducible nitric oxide synthase); 5'-AGCCGGGACTTCATCAATCAG-3' and 5'-GCCCAAACACCAGTCACTCTC-3' for eNOS (endothelial nitric oxide synthase); forward 5'-CTGATAACCTGGATGCAGTCGT-3',

Table 1. Hemodynamic and lipid profiles in this study.

	CTR (n=8)	CA (n=8)	CA+ATR (n=8)	P-value
RBC ($\times 10^{12}/L$)	8.39 \pm 0.90	8.28 \pm 0.38	8.12 \pm 0.23	0.338
Haemoglobin (g/L)	153.00 \pm 7.23	155.50 \pm 4.65	154.50 \pm 2.12	0.136
WBC ($\times 10^9/L$)	12.60 \pm 5.76	12.03 \pm 2.26	11.80 \pm 1.10	0.825
Platelets ($\times 10^9/L$)	949.25 \pm 98.34	828.50 \pm 138.11	895.50 \pm 140.74	0.701
TC (mg/dl)	70.1 \pm 5.6	73.1 \pm 2.3	69.1 \pm 3.5	0.120
TG (mg/dl)	74.3 \pm 5.1	76.8 \pm 6.2	78.2 \pm 4.3	0.487

**Figure 3.** The systemic blood pressure in rats with or without ATR treatment (A). The level of circulating EPC 3 months post CA induction surgery (B). Data are presented as mean \pm SD (n=6). ** P<0.01 vs. CA group.

reverse 5'-CCAGCCAGTCCGATTGA-3' for MMP-2 (matrix metalloproteinase-2); forward 5'-TTCAAGGACGGTCGGTATT-3', reverse 5'-CTCGAGCCTAGACCCAACCTTA-3' for MMP-9 (matrix metalloproteinase-9); forward 5'-AAGAAGGTGGTGAAGCAGGC-3', reverse 5'-TCCACCACCTGTT GCTGTA-3' for GAPDH (internal control). The mRNA content was normalized to GAPDH mRNA level and expressed as fold change relative to control levels. All reactions were performed in triplicate.

Statistical analysis

The IEL score was expressed as 95% CI for the median and was analyzed using the Siegel-Tukey test. For analysis of the other values (mean \pm SD), one-way analysis of variance followed via Bonferroni correction was used for multiple comparisons and the *t* test was used for comparisons between 2 groups. P<0.05 was set as the level of statistical significance.

Results

Influence of ATR on physiological parameters

There was no significant difference in red blood cell (RBC), hemoglobin, white blood cell (WBC), platelets, total cholesterol (TC), and triglyceride (TG) among CTR, CA, and CA+ATR groups (Table 1). Compared with the CTR group, systemic blood pressure of rats in the CA and CA+ATR groups was significantly higher at 1 month after CA induction (n=8; P<0.01; Figure 3A) and returned to the baseline level of the CTR group 3 months after CA induction. No difference was found in blood pressure between CA and CA+ATR groups throughout the course of the experiment.

ATR mobilized EPC

Compared with the CTR group, EPC level was markedly decreased 3 months after CA induction in the CA group ($34.3 \pm 10.8/2 \times 10^5$ MNCs vs. $59.3 \pm 7.3/2 \times 10^5$ MNCs, n=6; P<0.01; Figure 3B). ATR treatment after CA induction significantly raised the level of circulating EPC compared with the CA group ($95.7 \pm 11.1/2 \times 10^5$ MNCs vs. $59.3 \pm 7.3/2 \times 10^5$ MNCs, n=6; P<0.01).

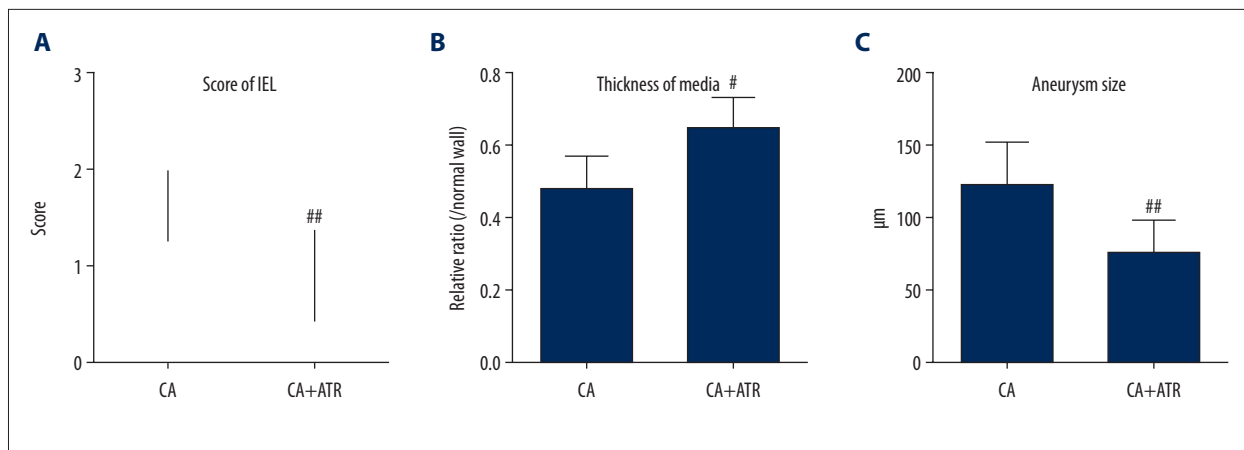


Figure 4. ATR treatment inhibited aneurysmal degeneration. Graphs showing IEL score (A; n=6), media thickness (B; n=6), and CA size (C; n=6). IEL scores are expressed as 95% CI for the median and other values are shown as mean ±SD, # P<0.05 vs. CA group, ## P<0.01 vs. CA group.

ATR protected against vascular degeneration after CA induction

To investigate the effect of ATR on aneurysmal degeneration, we performed Verhoeff-Van Gieson staining. The IEL score, media thickness, and CA size were evaluated by independent blinded investigators. Compared with the CA rats, ATR-treated CA rats had lower IEL score [(1.25–2.00) vs. (0.43–1.33), 95% CI for the median; n=6; P<0.01; Figure 4A], thicker medial layer (0.48±0.09 vs. 0.65±0.09, n=6; P<0.05; Figure 4B), and smaller CA size (123.5±28.4 µm vs. 74.79±22.8 µm, n=6; P<0.01; Figure 4C) 3 months after CA induction.

We further used TEM to observe the ultrastructure alteration of the aneurysmal wall in rats with or without ATR treatment. TEM observation showed that the normal ultrastructure of the cerebral artery wall (n=5; Figure 5A1, 5A2) was replaced by a severely degenerated vascular wall 3 months after CA induction, characterized by complete disappearance of endothelial cells (ECs) and IEL, damaged SMC in irregular arrangement, and degraded adventitial tissue (n=5; Figure 5B1, 5B2). In ATR-treated rats, ECs with nucleus and irregular IEL could be seen at the luminal surface of cerebral artery, but it was not continuous. SMC was partly preserved and arranged more regularly than that in the CA group. SMC could be distinguished from adventitial tissue (n=5; Figure 5C1, 5C2).

Effect of ATR on the expression of NF-κB, iNOS, eNOS, and MMP-2/9 gene in aneurysmal wall

We evaluated the expression profile of pathogenesis-related genes of CA using RT-PCR (Figure 6). *Fi* Quantification analysis showed that the expression of NF-κB (n=5; P<0.01), iNOS (n=5; P<0.01), MMP-2 (n=5; P<0.01), and MMP-9 (n=5; P<0.01) mRNAs were significantly upregulated, while the expression of eNOS

(n=5; P<0.01) mRNA was notably downregulated 3 months after CA induction. Compared with the CA group, ATR treatment following CA induction reversed the expression pattern of NF-κB (n=5; P<0.01), iNOS (n=5; P<0.01), eNOS (n=5; P<0.01), MMP-2 (n=5; P<0.01), and MMP-9 (n=5; P<0.01) mRNAs.

Discussion

Aneurysmal rupture is a major problem in CA patients, and surgical clipping and endovascular therapy are recommended in the standard guidelines for management of unruptured CA [17]. Because these invasive procedures potentially cause serious complications [18], it is necessary to search for a non-invasive prevention strategy for high-risk CA patients. The present study demonstrated that endothelial damage induced by artery ligation operation and high-salt diet was protected by enhancement of EPC mobilization following ATR administration. Further, the degradation and thinning of media, and wall protrusion were inhibited by ATR. The histopathological improvement suggests a vasculoprotective role of ATR in the process of vascular remodeling after CA induction, which did not rely on the modulation of blood lipids and systemic blood pressure by ATR.

There are also some advantages of the use of statins in patients with ruptured cerebral aneurysms. The administration of ATR significantly protected against aneurysmal subarachnoid hemorrhage (SAH) by decreasing the occurrence of vasospasm [19]. Moreover, the administration of simvastatin can reduce post-SAH cognitive dysfunction [20]. Above all, investigations show the clear efficacy of statins in the management of patients with unruptured or ruptured cerebral aneurysm.

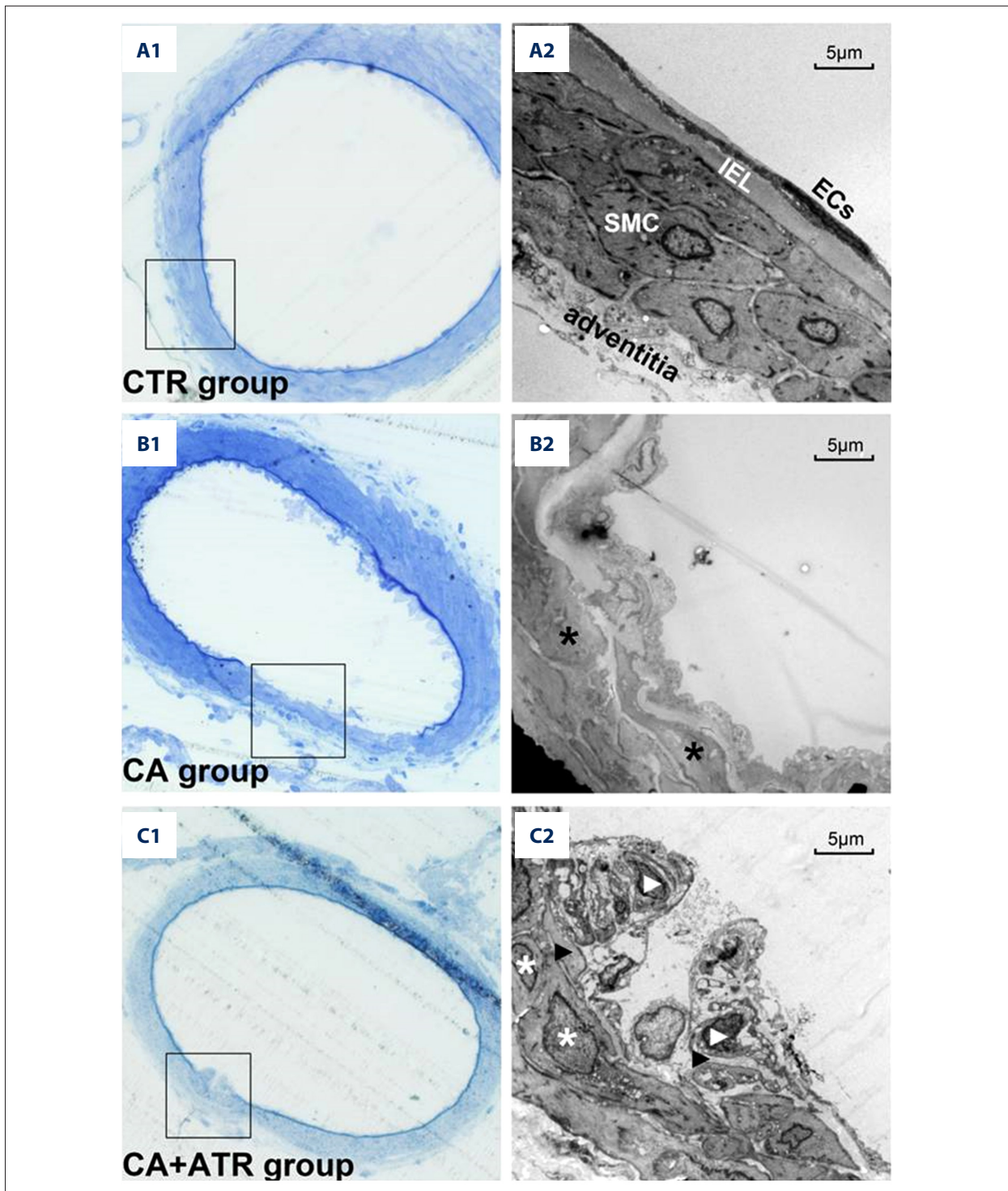


Figure 5. Transverse section of CA under light and transmission electron microscopy. Schematic representation of normal wall structure of cerebral artery, consisting of endothelial cells (ECs), continuous internal elastic lamina (IEL), regularly arranged smooth muscle cells (SMC), and adventitia (**A1, A2**). The ultrastructure of the aneurysmal wall in rat without ATR treatment 3 months after CA induction surgery. The degenerated and thinning wall was composed mainly of severely damaged SMC (black asterisk) and degraded adventitia, and ECs completely disappeared (**B1, B2**). Schematic representation of preserved vascular wall by ATR treatment (**C1, C2**). ECs with nucleus (white arrowhead), irregular IEL (black arrowhead), and SMC (white asterisk) were partly preserved and can be seen. Scale bar=5 μ m.

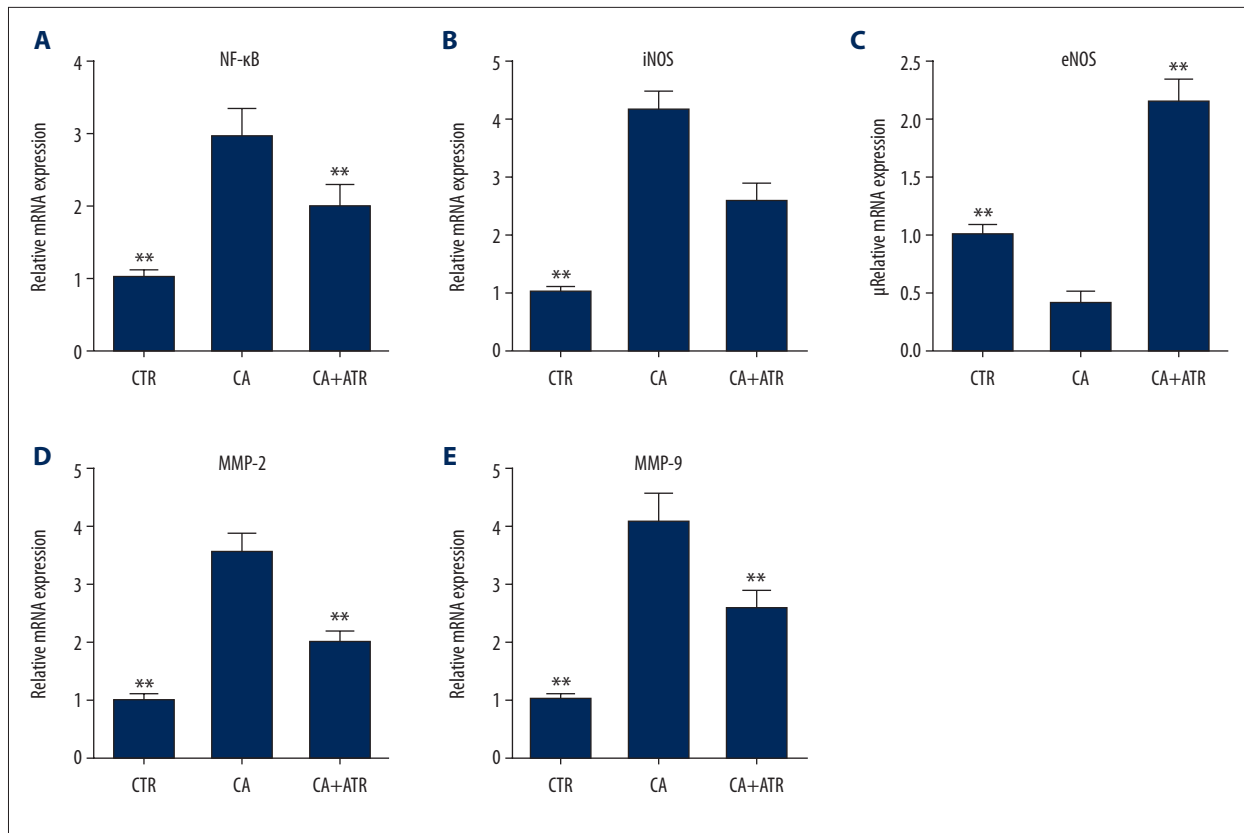


Figure 6. (A–E) Effect of ATR treatment on the gene expression of NF-κB, iNOS, eNOS, MMP-2, and MMP-9 in tissue of aneurysmal wall. Data were normalized to GAPDH mRNA levels and expressed as fold change relative to control levels. Values are shown as mean \pm SD of 5 independent experiments. ** $P < 0.01$ vs. CA group.

The correlation between EPC number and functional activity and cardiovascular disease is well documented. As an endogenous repair mechanism, circulating EPC maintains the integrity and normal function of the endothelium monolayer. Experimental and clinical studies have demonstrated that the number and function of EPCs are impaired in vascular disease [8,9,21], which aggravates the ECs injury and vascular degeneration. Sobrino et al. found that ATR treatment during the acute phase increased the levels of circulating EPC in patients with ischemic stroke [22]. Vasa et al. demonstrated that ATR increased the level of circulating EPC in patients with stable coronary artery disease (CAD) as early as 1 week after initiation of ATR treatment, and the EPC level increased by approximately 3-fold throughout the 4-week study period [23]. Previous studies have found that EPC derived from bone marrow are involved in the repair and remodeling processes, and participate in neointima formation and reendothelialization of aneurysm repair in elastase-induced carotid aneurysm in a rabbit model [24]. Oikonomou et al. showed that ATR treatment, beyond its lipid-lowering role, restored endothelial function due to EPC mobilization in patients with ischemic heart failure [11]. In line with previous studies, our results showed that ATR enhanced EPC mobilization in CA rats, which occurred independently of alteration in lipid level.

Endothelial injury is not only a biomarker for prediction of atherosclerotic disease progression [25], but is also an early and crucial event in the pathogenesis of CA [23]. The morphologic characteristics of ECs change in response to high shear stress. ECs elongate and orient to the direction of flow without high spatial shear stress gradient [26]. ECs change from a fusiform to column shape and gaps between ECs become wider [27], which may be attributable to decreased expression of junction proteins (VE-cadherin, occludin, and ZO-1) [28]. Our study provides evidence that ATR limits the destruction of ECs caused by shear stress. In addition to morphological changes, ECs exposed to high shear stress also undergo functional transition. The effects of atorvastatin on inflammation-related gene have been illustrated in human peripheral blood lymphocytes. A previous investigations showed that the expression the levels of inflammation-related factors CCL13, IL-8, PAI-1, and TGF-2 mRNA were significantly decreased by administration of atorvastatin [29]. Therefore, statins can inhibit the expressions of inflammation genes and play a role in preventing cardiovascular diseases.

Aoki et al. demonstrated that shear stress induced NF-κB activation in ECs [5]. As a transcriptional factor, NF-κB participates

in regulation of the expression of adhesion molecule, monocyte chemoattracting protein, iNOS, and MMPs. Nitric oxide (NO) and eNOS play a crucial role in vasorelaxation and inhibition of leukocyte-endothelial adhesion [30]. eNOS is also reported to be required for statin-induced improvement of EPC mobilization in experimental myocardial infarction [31]. Recent studies show that under shear stress, dysfunctional ECs exhibit downregulation of eNOS and decreased NO bioavailability [23]. All these morphological and functional changes of ECs are responsible for the initiation and progression of vascular inflammation and degeneration. Our present results show that ATR protects against ECs dysfunction, decreases the upregulation of NF- κ B, iNOS, and MMPs, and upregulates eNOS expression 3 months after CA induction.

In this preliminary study, it should be noted that using this established CA model we only investigated the effect of ATR on aneurysmal degeneration 3 months after surgery, at which

time the wall of OA/ACA bifurcation degenerates and develops into mature saccular CA. We directly used 3 mg/kg/day ATR with angiogenesis-promoting activity instead of examining the dose-dependent effect. In this study, 3 mg/kg/day ATR is low-dose atorvastatin. Moreover, the lipid profile tends to decrease after administration of ATR. Owing to a relatively short period of administration, there was no significant difference among the 3 groups. Further study is needed to understand the exact effect of long-term ATR administration on blood lipid.

Conclusions

ATR mobilized EPC and attenuated visible endothelial injury after CA induction, which consequently inhibited destruction and remodeling of the aneurysmal wall. These findings suggest that ATR is a promising noninvasive prevention strategy for CA.

References:

- Shimamura N, Ohkuma H: Phenotypic transformation of smooth muscle in vasospasm after aneurysmal subarachnoid hemorrhage. *Transl Stroke Res*, 2014; 5: 357–64
- Shimamura N, Naraoka M, Matsuda N et al: Prophylactic intra-arterial injection of vasodilator for asymptomatic vasospasm converts the patient to symptomatic vasospasm due to severe microcirculatory imbalance. *Biomed Res Int*, 2014; 2014: 382484
- Duvuru S, Sae-Ngow T, Kato Y et al: Does age affects the surgical outcome in patients with unruptured cerebral aneurysms? A 2-year retrospective study from a single center in Japan. *Asian J Neurosurg*, 2018; 13: 1108–11
- Mandelbaum M, Kolega J, Dolan JM et al: A critical role for proinflammatory behavior of smooth muscle cells in hemodynamic initiation of intracranial aneurysm. *PLoS One*, 2013; 8: e74357
- Aoki T, Nishimura M, Matsuoka T et al: PGE(2)-EP(2) signalling in endothelium is activated by haemodynamic stress and induces cerebral aneurysm through an amplifying loop via NF-kappaB. *Br J Pharmacol*, 2011; 163: 1237–49
- Sobhan PK, Seervi M, Joseph J et al: Immortalized functional endothelial progenitor cell lines from umbilical cord blood for vascular tissue engineering. *Tissue Eng Part C Methods*, 2012; 18: 890–902
- Balaji S, King A, Crombleholme TM, Keswani SG: The role of endothelial progenitor cells in postnatal vasculogenesis: implications for therapeutic neovascularization and wound healing. *Adv Wound Care (New Rochelle)*, 2013; 2: 283–95
- Wei H, Mao Q, Liu L et al: Changes and function of circulating endothelial progenitor cells in patients with cerebral aneurysm. *J Neurosci Res*, 2011; 89: 1822–28
- Xu Y, Tian Y, Wei HJ et al: Erythropoietin increases circulating endothelial progenitor cells and reduces the formation and progression of cerebral aneurysm in rats. *Neuroscience*, 2011; 181: 292–99
- Yoder MC, Mead LE, Prater D et al: Redefining endothelial progenitor cells via clonal analysis and hematopoietic stem/progenitor cell principals. *Blood*, 2007; 109: 1801–9
- Oikonomou E, Siasos G, Zaromitidou M et al: Atorvastatin treatment improves endothelial function through endothelial progenitor cells mobilization in ischemic heart failure patients. *Atherosclerosis*, 2015; 238: 159–64
- Hibbert B, Simard T, Ramirez FD et al: The effect of statins on circulating endothelial progenitor cells in humans: A systematic review. *J Cardiovasc Pharmacol*, 2013; 62: 491–96
- Rodriguez JN, Hwang W, Horn J et al: Design and biocompatibility of endovascular aneurysm filling devices. *J Biomed Mater Res A*, 2015; 103: 1577–94
- Li J, Zhang P, Wu S et al: Factors associated with favourable outcome in large hemispheric infarctions. *BMC Neurol*, 2018; 18: 152
- Liu L, Wei H, Chen F et al: Endothelial progenitor cells correlate with clinical outcome of traumatic brain injury. *Crit Care Med*, 2011; 39: 1760–65
- Aoki T, Nozaki K: Preemptive medicine for cerebral aneurysms. *Neurol Med Chir (Tokyo)*, 2016; 56: 552–68
- Thompson BG, Brown RD Jr, Amin-Hanjani S et al: Guidelines for the management of patients with unruptured intracranial aneurysms: A guideline for healthcare professionals from the American Heart Association/American Stroke Association. *Stroke*, 2015; 46: 2368–400
- Schetelig D, Frolich A, Knopp T, Werner R: A new cerebral vessel benchmark dataset (CAPUT) for validation of image-based aneurysm deformation estimation algorithms. *Sci Rep*, 2018; 8: 15999
- Shen J, Huang KY, Zhu Y et al: Effect of statin treatment on vasospasm-related morbidity and functional outcome in patients with aneurysmal subarachnoid hemorrhage: A systematic review and meta-analysis. *J Neurosurg*, 2017; 127: 291–301
- Merlo L, Cimino F, Scibilia A et al: Simvastatin administration ameliorates neurobehavioral consequences of subarachnoid hemorrhage in the rat. *J Neurotrauma*, 2011; 28: 2493–501
- Ruan C, Shen Y, Chen R et al: Endothelial progenitor cells and atherosclerosis. *Front Biosci (Landmark Ed)*, 2013; 18: 1194–201
- Sobrinho T, Blanco M, Perez-Mato M et al: Increased levels of circulating endothelial progenitor cells in patients with ischaemic stroke treated with statins during acute phase. *Eur J Neurol*, 2012; 19: 1539–46
- Budzyn M, Gryszczynska B, Majewski W et al: The association of serum thrombomodulin with endothelial injuring factors in abdominal aortic aneurysm. *Biomed Res Int*, 2017; 2017: 2791082
- Fang X, Zhao R, Wang K et al: Bone marrow-derived endothelial progenitor cells are involved in aneurysm repair in rabbits. *J Clin Neurosci*, 2012; 19: 1283–86
- Gutierrez E, Flammer AJ, Lerman LO et al: Endothelial dysfunction over the course of coronary artery disease. *Eur Heart J*, 2013; 34: 3175–81
- Sakamoto N, Saito N, Han X et al: Effect of spatial gradient in fluid shear stress on morphological changes in endothelial cells in response to flow. *Biochem Biophys Res Commun*, 2010; 395: 264–69
- Li MH, Li PG, Huang QL, Ling J: Endothelial injury preceding intracranial aneurysm formation in rabbits. *West Indian Med J*, 2014; 63: 167–71
- Tada Y, Yagi K, Kitazato KT et al: Reduction of endothelial tight junction proteins is related to cerebral aneurysm formation in rats. *J Hypertens*, 2010; 28: 1883–91
- Souza-Costa DC, Sandrim VC, Lopes LF et al: Anti-inflammatory effects of atorvastatin: modulation by the T-786C polymorphism in the endothelial nitric oxide synthase gene. *Atherosclerosis*, 2007; 193: 438–44
- Kim S, Woo CH: Laminar flow inhibits ER stress-induced endothelial apoptosis through PI3K/Akt-dependent signaling pathway. *Mol Cells*, 2018; 41: 964–70
- Guber S, Ebrahimian T, Heidari M et al: Endothelial nitric oxide synthase overexpressing human early outgrowth cells inhibit coronary artery smooth muscle cell migration through paracrine functions. *Sci Rep*, 2018; 8: 877